Journal of Biomedical Optics 6(3), 344–350 (July 2001)

Erbium: yttrium–aluminum–garnet laser induced vapor bubbles as a function of the quartz fiber tip geometry

Michael Mrochen
Peter Riedel
UKCGC, Technical University of Dresden
Department of Opthalmology
Fetscherstr. 74
01307 Dresden, Germany

Christof Donitzky
Wavelight Laser Technologie AG
Erlangen, Germany

Theo Seiler
UKCGC, Technical University of Dresden
Department of Opthalmology
Fetscherstr. 74
01307 Dresden, Germany

Abstract. Background. The use of modern erbium: yttrium–aluminum–garnet (YAG) laser systems in opthalmic microsurgery requires a precise knowledge of the size and dynamics of the laser induced vapor bubbles. The aim of this work was to clarify the possibilities of controlling the vapor bubble shape and size by using an optimized fiber tip geometry for various ophthalmic applications with the erbium: YAG laser. Methods. The mid-infrared radiation of free-running erbium: YAG laser was coupled optically into means of different low OH^- quartz fiber tips to investigate the vapor bubble formation in water by high-speed photography. The core diameter of four fiber tips ranged from 200 up to 940 μm. Fourteen fiber tips were polished at an angle graduated from 10° to 70° over the full core diameter (seven fiber tips) and over the half core diameter (seven fiber tips). Three fiber tips were produced to have a curvature at the distal end with curvature radii of 160, 230, and 420 μm. Results. The shape as well as the size of erbium: YAG laser induced vapor bubbles can be controlled systematically by using adequate fiber tip geometries. In detail, the used different angles and curvatures demonstrate that the propagation direction of the vapor bubbles can be estimated by optical modeling considering Snell's law and the Fresnel laws at a quartz-air boundary. Beside this, the size of a vapor bubble can be predetermined by choosing ideal fiber tip geometries to reduce or increase the radiant exposure at the distal end of the quartz fiber tip. Conclusions. The good possibility of controlling the shape and size of vapor bubbles offers a wider range of new applications, especially in ophthalmic microsurgery such as erbium YAG laser vitrectomy. [DOI: 10.1117/1.1381052]

Keywords: erbium: YAG laser; vapor bubble formation; laser-tissue interaction; ophthalmic microsurgery.

Paper 90066 received Dec. 20, 1999; revised manuscript received Jan. 24, 2001; accepted for publication Feb. 9, 2001.

1 Introduction

Mid-infrared lasers emitting near the 3 μm absorption peak of water have become a feasible tool for biological tissue ablation. In detail, the erbium: YAG laser emitting at a wavelength of 2.94 μm was purposed to be ideally suited for underwater tissue ablation because the absorption coefficient of water was reported to be around $10^4\ cm^{-1}$ at this wavelength.[1]

Combined with a fiber delivery system, the erbium: YAG laser seems to be a good choice for microsurgery procedures. In particular, this mid-infrared laser is useful for various applications in ophthalmology such as sclerostomy and trabecolectomy in glaucoma treatment, phacoemulsification in cataract surgery as well as in posterior segment surgery for removal of vitreous structures.[2–13]

Beside the precise tissue ablation, due to the high absorption in water containing tissue, microsurgical applications of pulsed erbium: YAG lasers require flexible (such as low OH^- quartz fibers) and high transparent optical waveguides (such as ZrF_4 fibers) for efficient light transmission that do not hinder surgeons. While standard low OH^- quartz fibers are not sufficiently transparent (attenuation 100 dB/m) to guide 2.94 μm radiation, the ZrF_4 fibers with an attenuation of less than 0.1 dB/m seem to be most applicable. However, the hydroscopic properties of the ZrF_4 fibers require protection against contamination of aqueous solutions. Thus, several commercial available erbium: YAG laser systems are using ZrF_4 fibers to transmit the mid-infrared radiation to an application handpiece and within the handpiece the radiation is coupled optically into interchangeable low OH^- quartz fiber tip with a length of a few centimeters.

An additional difficulty of microsurgical applications of the erbium: YAG laser in ophthalmology is that the freedom

Dr. Mrochen is scientific consultant of the WaveLight Laser Technologie AG, Erlangen, Germany. Parts of this work were presented at the SPIE Meeting, BIOS 1990; Proceedings Ophthalmic Technologies, San Jose, Vol. 3591, pp. 171–181. Address all correspondence to Michael Mrochen, Ph.D. Tel: ++411-255-4993; Fax: ++411-255-4472; E-mail: michael.mrochen@aug.usz.ch

1083-3668/2001/$15.00 © 2001 SPIE

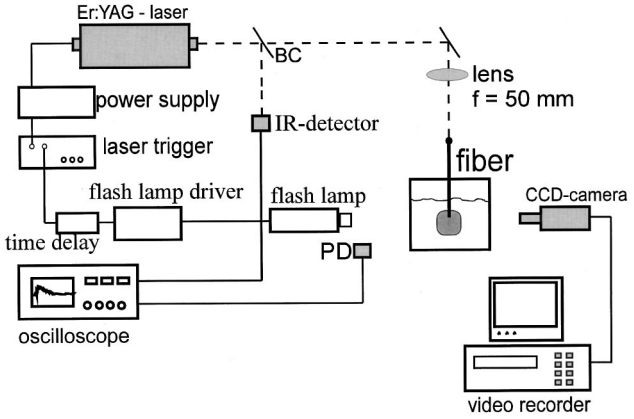

Fig. 1 Scheme of the experimental setup to investigate the vapor bubble formation. PD: Photodetector with a time resolution of less than 1 ns to measure the laser pulse duration of the erbium:YAG laser.

of movement is limited to a few millimeters or less, and the tissue that has to be irradiated is usually not in an axial direction to the fiber application.

The aim of this work was to investigate the dependence of the vapor bubble formation on the geometry of means of low OH^- quartz fiber tips as they might be useful for ophthalmic microsurgery with the erbium: YAG laser.

2 Materials and Methods

The used free-running erbium: YAG laser (WaveLight Laser Technologie GmbH, Erlangen, Germany) was emitting pulse durations in the range of 100–200μs [full width at half maximum (FWHM)], a pulse energy of 50 mJ, and the repetition rate of the erbium: YAG laser was chosen to be 10 Hz. Here, the laser energy was coupled into means of low OH^- quartz fiber tips (length 42 mm) by an Infrasil lens (focal length $f = 50$ mm). The distal fiber tips were positioned in an optical cuvette (dimensions $20\times30\times20$ mm^3) filled with de-ionized water at room temperature. The fiber tips were kept at least 1 cm below the water surface to insure sufficient inertial confinement. A scheme of the experimental setup is shown in Figure 1.

An area of approximately 4×5 mm around the distal fiber tip was illuminated by a fast flash lamp (High-Speed Photo-Systeme, Wedel, Germany) with a pulse duration of 20 ns.

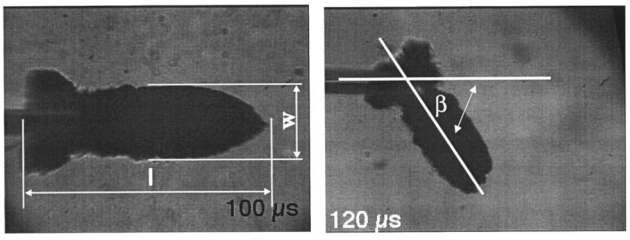

Fig. 2 Determination of the evaporation bubble size; 1 holds for the length and w for the width of the vapor bubble at a time delay of 100 μs for a plane fiber tip (left) and 120 μs for a polished fiber tip with an angle α of 60° (right). The core diameter of the fiber tips was 320 μm, the laser pulse duration 160 μs, and the laser pulse energy 50 mJ at the distal end of the fiber.

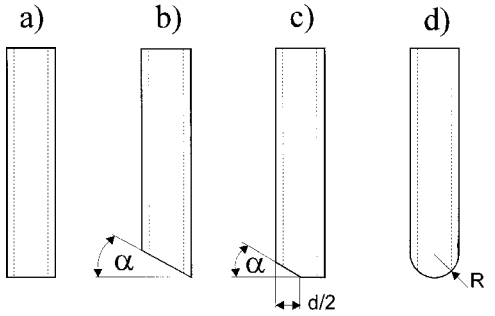

Fig. 3 Scheme of the quartz fiber tips with different polished distal sides. (a) Plane, (b) polished angle, (c) half plane and (d) curvature. The angle α and the radius of the curvature R were polished by means of quartz fiber tips (core diameter 320 μm). The outer diameter of the fiber tip was 380 μm.

The emitted light was homogenized by a light shaping beam homogenizer[14] and collimated by a quartz lens. The flash lamp was synchronized with the IR laser by means of trigger and delay units to permit flash photographs to be taken at variable delay times of 0 μs up to 2 ms after the start of the initial IR laser pulse.

The delay time was monitored with an oscilloscope by measuring the laser pulse and the flash lamp by means of a photodetector (PEM-L-3, DoroTek, Berlin, Germany) with a time resolution of 1 ns. A sequence of pictures of the bubble formation was recorded by varying the delay time between the IR laser pulses and the flash lamp. The length and width (FWHM) of the vapor bubbles were determined by the analysis of images recorded with a charge coupled device camera as shown in Figure 2. The maximum bubble size (length and width) was derived from the dependence of the bubble size (averaged over 10 measurements) on the delay time.

An overview of the used fiber tip geometries is given in Figure 3 and a detailed discription is shown in Table 1. Besides the variation of the fiber tip core diameter, the distal ends of means of quartz fiber tips were polished at the full or half diameter at an angle α ranging from 0° up 70° [Figures 3(b) and 3(c)]. The distal ends of three quartz fiber tips were polished at a curvature radius $R = 160$, 230, and 420 μm [Figure 3(d)]. To compare the radii of the different curvatures we

Table 1 Overview of the used fiber tip geometries.

Geometry	Diameter [μm]	Angle α [°]	Optical refraction D [1/m]
Plane	200, 320, 550, 900	0°	…
Angle	320	0°, 10°, 20°, 30°, 40°, 50°, 60°, 70°	…
Half angle	320	0°, 10°, 20°, 30°, 40°, 50°, 60°, 70°	…
Curvature	320	…	0, 1000, 2100, 3000

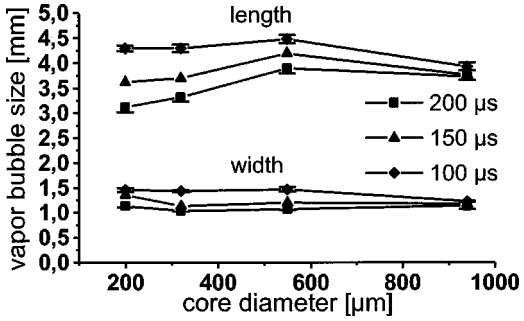

Fig. 4 Maximum vapor bubble size as a function of the core diameter of the quartz fiber tip for different laser pulse durations. The laser pulse energy was 50 mJ and the core diameters were 200, 320, 550, and 940 μm.

used the optical refraction $D=(n-1)/R$ with $n=1.42$ the refractive index of quartz at a wavelength of 2.94 μm.[15]

3 Results

Figure 4 demonstrates the dependence of the vapor bubble width (FWHM) and length as a function of core diameter of the quartz fiber tip. Increasing the core diameter of the tip from 200 up to 940 μm does not change the width or length of the vapor bubble significantly. However, the high speed photographies of the vapor bubble at 100 μs delay time demonstrate a change in the shape of the observed bubbles (Figure 5). At a core diameter of 200 μm the vapor bubbles show a cylindrical shape, where the shape of the vapor bubbles for 940 μm are more triangular shaped. Increasing the laser pulse duration from 100 up to 200 μs results in a decrease of the maximum vapor bubble length from 3 up to 4.5 mm at a core diameter of 200 μm (Figure 4). However, at a core diameter to 940 μm the maximum vapor bubble size yields to be independent from the change of the laser pulse duration.

A sequence of vapor bubbles at different polished angles α is presented in Figure 6. These side view pictures demonstrate that the radiation leaves the fiber tip only appropriate to the

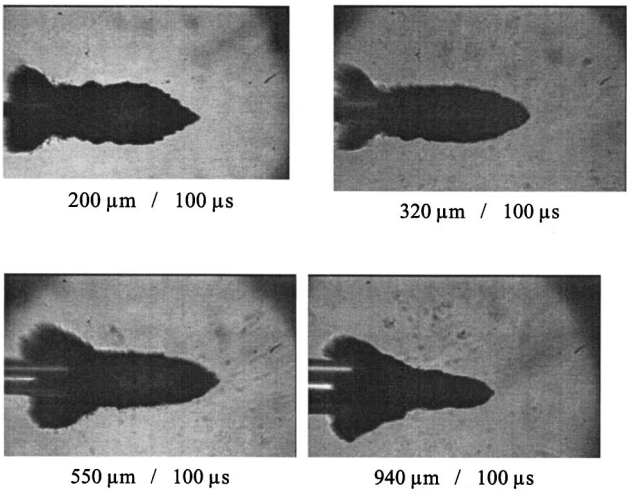

Fig. 5 Sequence of the vapor bubble formation for different diameters of the fiber tip. The laser pulse duration was 160 μs and the laser pulse energy 50 mJ at the distal end of the fiber.

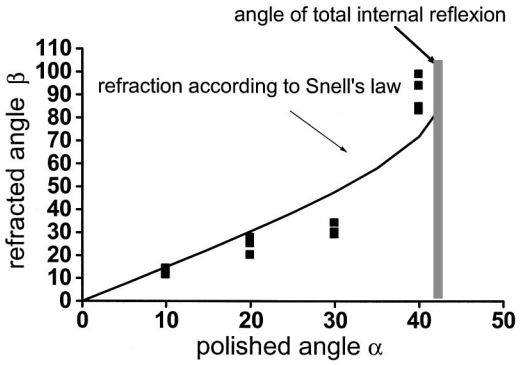

Fig. 6 Sequence of the vapor bubble formation for different polished angles α. The core diameter of the fiber tips was 320 μm. The laser pulse duration was 160 μs and the laser pulse energy was 50 mJ at the distal end of the fiber.

optical pathway of the light at the quartz-vapor boundary. Varying the polished angles α from 0° up to 70°, we found two conditions for the propagation of the vapor bubbles: (1) For angles α that are smaller than the angle of total internal reflection $\alpha_{tot}=42.5°$, the radiation was refracted according to Snell's law at the boundary between the quartz tip and the vapor that was formed after the first few microseconds of the laser pulse (see Figure 7). (2) For angles $\alpha>\alpha_{tot}$, the radiation was reflected according to Fresnel laws at the boundary between the quartz tip and the vapor. Surprisingly, a splitting of the vapor bubble into three parts can be observed for angles in the range of the angle of total internal reflection α_{tot} as well as a nearly spherical vapor bubble at an angle of $\alpha=70°$. These effects are a result of multiple reflections and refractions within the quartz fiber tip at the quartz-vapor boundary.

A comparable situation can be observed by using the half plane geometry of the fiber tip (Figure 8). Here, the bubble was split into three parts: (1) propagation into the direction of a plane fiber; (2) propagation into the direction of total internal reflection, and (3) propagation into the direction of multiple internal reflections. Here, the major part of the vapor bubble was transmitted in prolongation through the fiber tip.

Figure 9 represents the typical bubble formation for fiber tips with a curvature at the distal. The bubble for a fiber with curvature shows a waist that is not present for a plane fiber tip. Furthermore, the vapor bubble yields to be shorter. Figure 10 quantifies this reduction of the vapor bubble length in dependence on the refraction of the quartz fiber tip. The width of the bubbles yields to be unchanged.

4 Discussion

The results of the present study demonstrate the possibility of controlling the vapor bubbles induced by erbium:YAG laser radiation by means of distal ends of low OH^- quartz fiber tips. Basically, the propagation direction of the vapor bubbles belongs to the optical principles such as refraction and reflection at a quartz-air boundary. Thus, Snell's law as well as the Fresnel laws can be used to predetermine the propagation direction of such vapor bubbles.

Jansen and co-workers[16] predicted in the case of a plane fiber the bubble dimensions based on a partial vaporization model and compared their theoretical results with experimen-

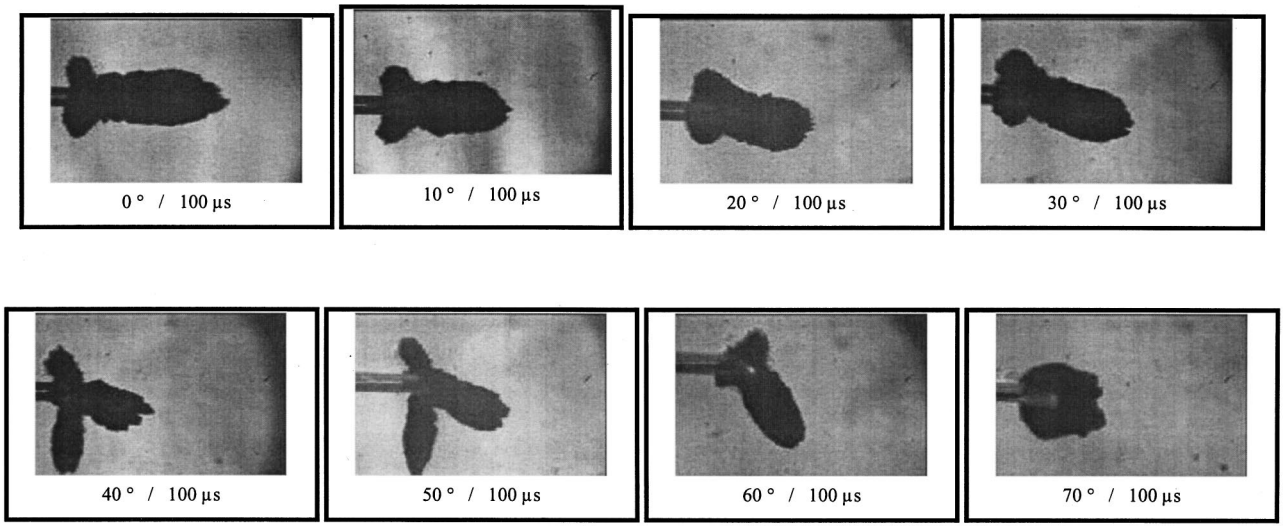

Fig. 7 Angle of the refracted vapor bubble β as a function of the polished angle of the quartz fiber tip. The bar represents the angle of total internal reflection at the quartz-air boundary. The vapor bubble is reflected at the polished side of the quartz fiber tip by angles greater than the angle of total internal reflection [see Figure 7(b)]. The core diameter of the fiber tips was 320 μm, the laser pulse duration was 160 μs, and the laser pulse energy 50 mJ at the distal end of the fiber.

tal findings obtained from a Ho:YAG laser (wavelength 2.1 μm). They have been shown, that the most convincing evidence for partial vaporization can be observed in the very early phase approximately 0.5 μs after the start of the laser pulse. Here, the initial vapor bubble formation takes place, not over the entire area of the fiber tip, but at nucleation sites in front of the fiber tip. Within a microsecond these bubblets coalesced to one single bubble which then started to grow to some maximum volume and eventually collapsed. They pointed out that the partial vaporization theory is in agreement with the phenomenon of homogeneous nucleate boiling of water by the 2.1 μm radiation. The absorption coefficient of water at a wavelength of 2.94 μm under steady state conditions is nearly 500 times higher than the absorption coefficient at 2.1 μm (absorptions coefficient 20 cm^{-1}).[1] The absorption peak of water at 3 μm, however, is known to be plagued with a bleaching effect due to the breaking of hydrogen bonds between the water molecules when the temperature is increased.[17] Furthermore, the nearly independent maximum length and width of the vapor bubbles seem to prove this description; here, one might estimate that the size or volume of the vapor bubbles does not depend on the entire area of the fiber tip, but even more on the laser pulse energy. Besides this, the size of the vapor bubbles decreases by increasing the laser pulse duration. It has to be mentioned, that for increasing pulse durations the vapor bubble channel closes and reopens

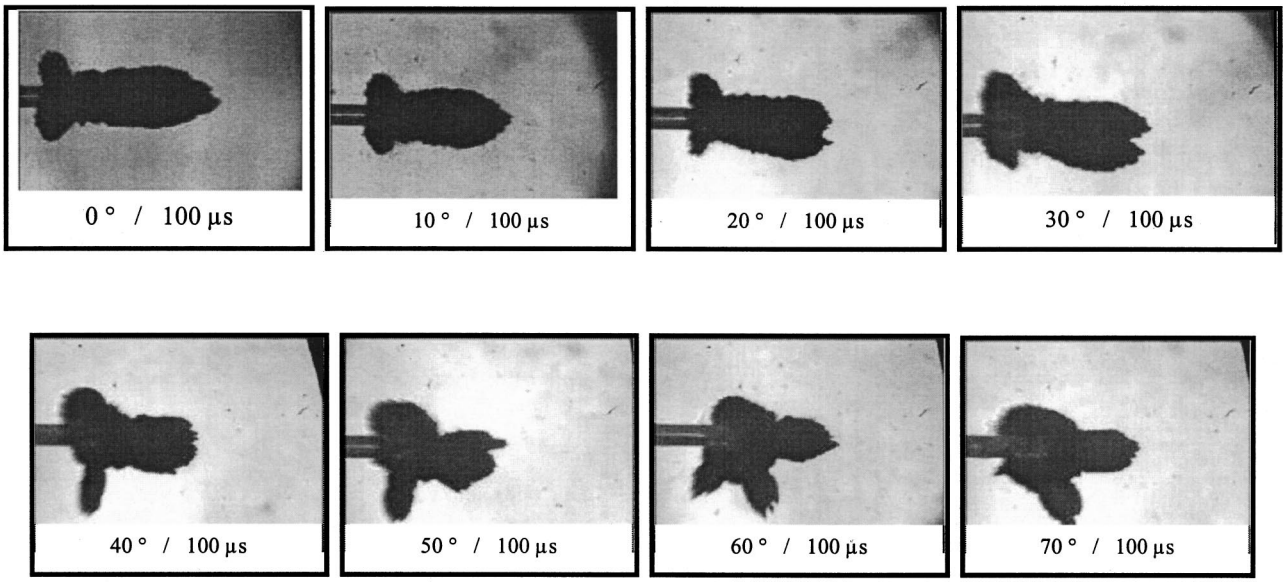

Fig. 8 Sequence of the vapor bubble formation for different polished angles α and the half plane geometry. The core diameter of the fiber tips was 320 μm, the laser pulse duration was 160 μs, and the laser pulse energy was 50 mJ at the distal end of the fiber.

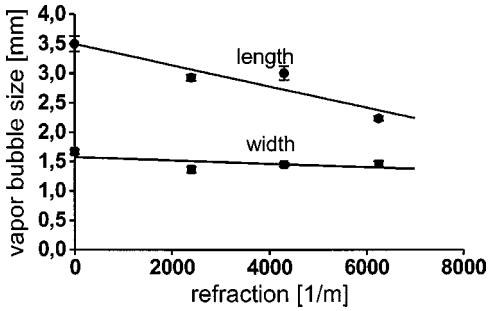

Fig. 9 Sequence of the vapor bubble formation for different refractions of the distal end of the fiber tip. The core diameter of the fiber tips was 320 μm, the laser pulse duration was 160 μs, and the laser pulse energy was 50 mJ at the distal end of the fiber.

during the laser pulse and this leads to a strongly decreasing fraction of the transmitted energy resulting in a decrease of the vapor bubble size.[18,19] Further studies should focus on the phenomenon of the bubble closing and reopening under different conditions such as incidence radiant exposure, optical, mechanical, and thermal properties of the liquid.[20,21,22] In addition, it must be clarified whether there is clinical relevance of this phenomenon in long and short range underwater tissue damage.

An additional result has been reported by Föhn et al.[15] in the case of a side-firing quartz fiber tip (polished angle 30°). They demonstrated that an erbium:YAG laser pulse generates randomly distributed microbubbles onto the distal surface of the angle fiber. At 10 μs after the beginning of the laser pulse a thin vapor layer has been formed throughout the angled surface and at the time the start of a vapor bubble on the side of the fiber tip could be observed. At 100 μs, an elongated channel was formed in a sideways direction at 44° relative to the fiber axis. These results are in good agreement with the results presented in this work, however, we could not find detailed investigations about the dependence of the vapor bubble formation on various fiber tip geometries in the literature.

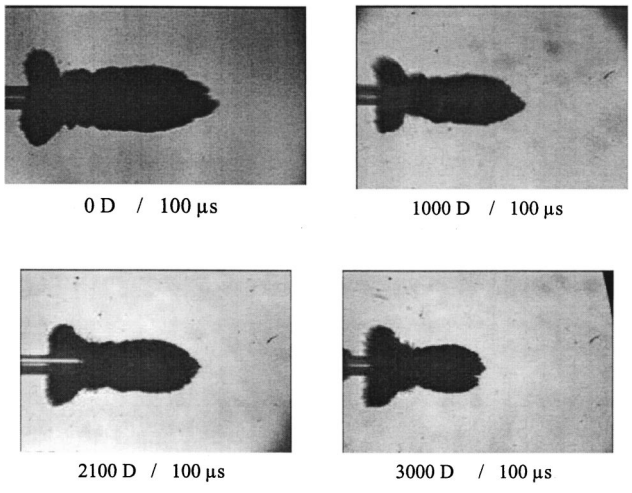

Fig. 10 Vapor bubble size as a function of the fiber tip refraction. The core diameter of the fiber tips was 320 μm, the laser pulse duration was 160 μs, and the laser pulse energy was 50 mJ at the distal end of the fiber.

The formation of a vapor bubble is used as a transmission channel for the infrared radiation between the fiber tip and the tissue surface that should be ablated.[15] This is possible because water vapor, in contrast to the liquid water, has first a lower density and second a smaller absorption coefficient at the 3 μm wavelength.[17] The formation and collapse of these vapor bubbles are both accompanied by pressure gradients and exhibit complex dynamics. The pressure transients induced by the bubble collapse are known to be an order of magnitude stronger than the pressure waves resulting from the explosive ablation process with free-running erbium:YAG lasers. However, the main bubbles collapse, often sending out multiple pressure waves of a spherical shape. The collapse velocity, and therefore the induced pressure, strongly depends on the volume and the geometry of the bubble, both of which depend on the laser pulse energy and pulse duration.[23] The more spherical the bubble, the stronger the resulting pressure signal. Future investigations should focus on this problem, whether the pressure transients are increasing or decreasing by changing the fiber tip geometry.

Various pre-clinical and clinical publications[2–13] have reported about the feasibility of using the erbium:YAG laser in different maneuvers in anterior and posterior surgery of the eye. However, the use of various fiber tip geometries might optimize or increase the field of erbium:YAG laser applications in ophthalmic microsurgery.

Dietlein and co-workers[4] demonstrated experimentally the need for larger core diameters to achieve larger ablation areas in the trabecular meshwork for open angle glaucoma treatment without augmentation of collateral tissue damage. Our results show, that there is no remarkable increase of the vapor bubble width by increasing the core diameter. However, a different situation might be observed when the fiber was placed close to the tissue so that photoablation can occur. Here, the tissue primarily depends on the radiant exposure and therefore a larger ablation diameter can be observed after laser treatment with a radiant exposure beyond the ablation threshold. Besides this, the dimensions of photoablated volume have been found to be not only dependent on the radiant exposure and specific tissue absorption, but also on simple mechanical forces along the longitudinal axis of the fiber tip that might lead to an enlargement of the photoablated tissue volume. The side-firing fiber tips with a polished angle at the distal end are, especially, very sharp and therefore they might be harmful for fragile tissue structures and should therefore be covered by a canula.

Some reports[5–8,24,25] investigated the use of pulsed erbium:YAG lasers as an alternative in phacoemulsification to liquefy the cataract lens of the eye. Basically, there are concerns over potential effects of ultrasonic energy delivery by the phacoemulsification probe on such nontarget ocular structures as the corneal endothelium and the lens capsule. Here, the erbium:YAG laser imparts less thermal energy to the entire eye than ultrasonic phacoemulsification.[26] The threshold for ablating altered lens structures has been investigated carefully to be in the range of 1–2 J/cm^2 by different authors.[5–7,27] Nevertheless, a major problem of erbium:YAG laser phacoemulsification seems to be the 4–5 times higher treatment time compared to the ultrasonic systems when using a core diam-

eter of 320 or 550 μm and a repetition rate of 70 Hz (Seiler and Mrochen; unpublished results 1998). In contrast to the technical difficulty of increasing the repetition rate, one might expect that a greater ablation volume per pulse is capable of overcoming this problem, i.e., a larger core diameter as well as an appropriate increase of the laser pulse energy should remove more lens structures with each laser pulse and this might result in a decrease of the treatment time. An increase of the core diameter from 320 up to 940 μm leads to an increase of the entire area of the fiber tip by a factor of 8.6, however, it can be easily approximated that the pulse energy should also be increased by this factor to insure a constant radiant exposure for lens tissue ablation. On the other hand, the radiant exposure at the lens tissue can be significantly increased by using a curvature at the distal end of the fiber tip.

Clinical studies of erbium:YAG laser vitrectomy and vitreoretinal surgery have documented the suitability of this laser for intraocular surgery.[11,13,28,29,30] In detail, the vitrectomy, a surgery technique to liquefy and aspirate vitreous structures, seem to be the most promising application of erbium:YAG lasers in ophthalmic microsurgery. Here, a small portion of the altered vitreous structures is sucked into a microsurgery probe with an outer diameter of 0.9 mm, cut by the erbium:YAG laser and then aspirated within the microsurgery probe from the eye. The laser radiation was transmitted inside the microsurgery probe by low OH^- quartz fiber tip to the distal end of the probe. Placing a fiber tip inside a microsurgery probe dose significantly changes the geometry of the vapor bubbles due to the small lumen of the microsurgery probe.[31] As a consequence, a spread out of the vapor bubble from the aspiration port (inner diameter 0.2–0.6 mm) of the microsurgery probe has been observed that might be harmful for the surrounding tissue. Therefore, the size of the vapor bubble should be as small and the radiant exposure should be as high as possible for reliable tissue cutting and this might be achieved by using a fiber tip with a curvature at the distal end. On the other hand, creating a more spherical bubble might result in the generation of unwanted large pressure transients and, thus, further work has to be performed for investigations on the dependence of the vapor bubble formation on the constructive geometries of the microsurgery probes.

In summary, we have demonstrated the possibility of optimizing quartz fiber tip geometries for controlling the laser induced vapor bubbles used in various ophthalmic microsurgery applications with the erbium:YAG laser. Basically, the propagation of such bubbles can be estimated by optical modeling considering Snell's law and the Fresnel laws at a quartz-air boundary. However, additional investigations are needed to clarify the effect of different fiber tip geometries on the pressure transients induced by the bubble collapse, the laser tissue interaction with different fiber geometries, as well as the influence of the microsurgery probe geometries on the vapor bubble formation. These investigations might help to find new applications or to optimize commonly used surgery techniques in ophthalmology with erbium:YAG laser.

Acknowledgments

This work was supported by the Brunenbusch-Stein Foundation and the WaveLight Laser Technologie GmbH, Erlangen, Tennenlohe.

References

1. G. M. Hale and M. R. Querry, ''Optical constants of water in the 200 nm to 200 μm wavelength region,'' *Appl. Opt.* **12**, 555–563 (1973).
2. S. A. Oezler, R. A. Hill, J. J. Andrews, G. Baerveldt, and W. M. Berns, ''Infrared laser sclerostomy,'' *Invest. Ophthalmol. Visual Sci.* **32**, 2498–2503 (1991).
3. W. Wetzel, R. Otto, W. Falkenstein, U. Schmidt-Erfurth and R. Birngruber, ''Development of a new Er:YAG laser conception for laser sclerostomy *ab externo*: experimental and first clinical results,'' *German J. Ophthalmol.* **4**, 283–288 (1995).
4. T. S. Dietlein, P. C. Jacobi, and G. K. Kriegelstein, ''Erbium:YAG laser ablation on human trabecular meshwork by contact delivery endoprobes,'' *Ophthalmic Surgery and Lasers* **27**, 939–945 (1996).
5. R. P. Gailitis, S. W. Patterson, M. A. Samuels, K. Hagen, Q. Ren, and G. O. Waring III, ''Comparison of laser phacovaporization using Er-YAG and the Er-YSGG laser,'' *Arch. Ophthalmol. (Chicago)* **111**, 697–700 (1993).
6. B. S. Ross and C. A. Puliafito, ''Erbium-YAG and Holmium-YAG laser ablation of the lens,'' *Lasers Surg. Med.* **15**, 74–82 (1994).
7. T. Bende, M. Kriegerowski, and T. Seiler, ''Photoablation in different ocular tissues performed with an Erbium:YAG laser,'' *Lasers Ophthalmol.* **2**, 263–269 (1989).
8. H. Höh and E. Fischer, ''Erbiumlaserphakoemulsifikation-Eine klinische Pilotstudie,'' *Klein Monatsbl Augenheilkd* **214**, 203–210 (1999).
9. P. D. Bazitikos, D. J. D'Amico, T. W. Bochow, M. Hmelar, G. R. Marcellino, and N. T. Stangos, ''Experimental ocular surgery with a high-repetition-rate Erbium:YAG laser,'' *Invest. Ophthalmol. Visual Sci.* **39**, 1667–1675 (1998).
10. T. I. Margolis, D. A. Farnath, M. Destor, and C. A. Puliafito, ''Erbium-YAG laser surgery on experimental vitreous membranes,'' *Arch. Ophthalmol. (Chicago)* **107**, 424–428 (1989).
11. D. J. D'Amico, M. S. Blumenkranz, M. I. Lavin, H. Quiroz-Mercado, I. G. Pallikaris, G. R. Marcellino, and G. E. Brooks, ''Multicenter clinical experience using an Erbium:YAG laser for vitreoretinal surgery,'' *Ophthalmology (Philadelphia)* **103**, 1575–1585 (1996).
12. M. Mrochen, H. Petersen, Ch. Wüllner, and T. Seiler, ''Experimentelle Ergebnisse zur Erbium:YAG-Laservitrektomie,'' *Klin Monatsbl Augenheilkd.* **212**, 50–54 (1998).
13. H. Petersen, M. Mrochen and T. Seiler, ''Comparison of Erbium:YAG—laser and mechanical vitrectomy—a clinical study,'' *Ophthalmology (Philadelphia)* **107**, 1389–1392 (2000).
14. M. Mrochen, V. Semchishen, V. Seminogov, and T. Seiler, ''Strahlhomogenisierung mittels definiertem statistischem Oberflächenrelief für medizinische Anwendung,'' *Laser Optoelektron.* **30**, 71–76 (1998).
15. O. Föhn, H. S. Pratisto, F. Könz, M. Ith, H. J. Altermatt, M. Frenz, and H. P. Weber, ''Side-firing fiber device for underwater tissue ablation with Ho:YAG and Er:YAG laser radiation,'' *J. Biomed. Opt.* **3**(1), 112–122 (1998).
16. D. E. Jansen, T. G. van Leeuwen, M. Motamedi, C. Borst, and A. J. Welch, ''Partial vaporization model for pulsed mid-infrared laser ablation of water,'' *J. Appl. Phys.* **78**, 564–571 (1995).
17. K. L. Vodopyanov, ''Bleaching of water by intense light at the maximum of the $\lambda = 3$ μm absorption band,'' *Sov. Phys. JETP* **70**, 114–121 (1990).
18. T. Assauer, K. Rink, and G. Delacretaz, ''Acoustic transient generation by holmium-laser-induced cavitation bubbles,'' *J. Appl. Phys.* **76**, 5007–5013 (1994).
19. M. Ith, H. Pratisto, H. J. Altermatt, M. Frenz, and H. P. Weber, ''Dynamics of laser-induced channel formation in water and influence of pulse duration on the ablation of biotissue under water with pulsed erbium-laser radiation,'' *Appl. Phys. B: Lasers Opt.* **59**, 621–629 (1994).
20. T. Wesendahl, P. Janknecht, B. Ott, and M. Frenz, ''Erbium:YAG laser ablation of retinal tissue under perfluorodecaline: determination of laser-tissue interaction in pig eyes.'' *Invest. Ophthalmol. Visual Sci.* **41**, 505–512 (2000).
21. M. Mrochen, P. Riedel, A. Kempe, and T. Seiler, ''Erbium:YAG—laser vitrektomie: temperaturmessungen in unterschiedlichen austauschmedien,'' *Der. Ophthalmologe.* **97**, 181–185 (2000).
22. H. Loertscher, W. O. Shi, and W. S. Grundfest, ''Tissue ablation throughout water with erbium: YAG lasers,'' *IEEE Trans. Biomed. Eng.* **39**, 86–88 (1992).
23. A. Vogel, R. Engelhardt, U. Behnle, and U. Parlitz, ''Minimization of

cavitation effects in pulsed laser ablation illustrated on laser angioplasty,'' *Appl. Phys. B: Lasers Opt.* **62**, 173–182 (1996).
24. W. Wetzel, R. Brinkmann, N. Koop, E. Schroer, and R. Birngruber, ''Photofragmentation of lens nuclei using the Er:YAG laser: preliminary report of an in vitro study,'' *Ger. J. Opthalmol.* **5**, 281–284 (1996).
25. H. Hoh and E. Fischer, ''Pilot study on erbium laser phacoemulsification,'' *Ophthalmology (Philadelphia)* **107**, 1053–1061 (2000).
26. J. W. Berger, J. H. Talamo, K. J. LaMarch, S.-H. Kim, R. W. Snyder, D. J. D'Amico, and G. Marcellino, ''Temperature measurements during phacoemulsification and erbium:YAG laser phacoablation in model systems,'' *J. Cataract Refractive Surg.* **22**, 372–378 (1996).
27. V. A. Mikhailov, V. B. Tsvetkov, and I. A. Shcherbakov, ''Investigation of potential medical applications of fiber-coupled lasers based on Er^{3+} and Ho^{3+} in Cr^{3+}-doped scandium garnet crystals,'' *Soc. Lightwave. Commun.* **2**, 13–22 (1992).
28. M. Krause, D. Steeb, H. J. Foth, J. Weindler, and K. W. Ruprecht, ''Ablation of vitreous tissue with erbium:YAG laser,'' *Invest. Ophthalmol. Visual Sci.* **40**, 1025–1032 (1999).
29. S. Binder, U. Stolba, L. Kellner, and I. Krebs, ''Erbium:YAG laser vitrectomy: clinical results,'' *Am. J. Ophthalmol.* **130**, 82–86 (2000).
30. P. Riedel, M. Mrochen, C. Donitzky, and T. Seiler, ''Bewegungsartifakte bei der Vitrektomie,'' *Der. Ophthalmologe.* **97**, 615–618 (2000).
31. C. P. Lin, D. Stern, and C. A. Puliafito, ''High-speed photography of Er:YAG laser ablation in fluid—implification for laser vitreous surgery,'' *Invest. Ophthalmol. Visual Sci.* **31**, 2546–2550 (1990).